A Waveform Design Methodology for UHF RFID Systems: A Hybrid Simulation Approach

Hussein Ezzeddine, Julien Huillery, Arnaud Bréard, Yvan Duroc

A Waveform Design Methodology for UHF RFID Systems: A Hybrid Simulation Approach

Hussein Ezzeddine*, Julien Huillery*, Arnaud Bréard* and Yvan Duroc†
* Univ Lyon, Ecole Centrale de Lyon, INSA Lyon, Université Claude Bernard Lyon 1, CNRS
Ampère, UMR5005, 69130 Ecully, France
Email: hussein.ezzeddine@ec-lyon.fr
† Univ Lyon, Université Claude Bernard Lyon 1, INSA Lyon, Ecole Centrale de Lyon, CNRS
Ampère, UMR5005, 69622 Villeurbanne, France
Email: yvan.duroc@univ-lyon1.fr

***Abstract*—In this paper, we propose a waveform design methodology for ultra high frequency radio frequency identification (UHF RFID) systems based on the quantitative analysis of the backscattered signal. This latter is leveraged to probe the wireless propagation channel, allocate power accordingly to frequency components, and design channel-adaptive multisine signals. UHF RFID system performance is evaluated based on the harvested DC voltage at the output of the rectifying circuit of the RFID tag. To this end, a flexible hybrid simulation model with modular architecture is developed via the ANSYS platform to study UHF RFID system performance. Simulation results show that the designed waveforms provide an improved energetic efficiency especially in highly reflective environments.**

***Index Terms*—UHF RFID, WPT, waveform design, multisine signals, adaptive power allocation, hybrid simulation.**

I. Introduction

Radio frequency identification (RFID) has nowadays become an indispensable wireless technology with applications spanning numerous aspects of the industry as well as our daily lives [1]. Contrary to conventional RF communications, passive ultra high frequency (UHF) RFID systems rely on wireless power transfer (WPT) and backscattering of electromagnetic waves to establish communication. However, this implies limited energy efficiency and read range, which is one of the main challenges for UHF RFID technology.

Waveform optimization for UHF RFID systems has gained significant attention in recent years as a solution to improve the read range of RFID tags. It has been widely adopted due to the different advantages it offers over other classical solutions, namely, improving the energetic efficiency of the reader-tag wireless communication link, compliance with the current EPC UHF Gen2 protocol [2], and compatibility with commercial RFID tags. To that extent, there has been several approaches to design optimized waveforms for efficient WPT. In [3]–[5] the approaches relied, in principle, on designing signals having high peak-to-average power ratio (PAPR) at emission to increase the energy efficiency of the communication link. In [6]–[10] channel-adaptive waveforms have been proposed where the exact channel state information (CSI) was assumed to be known to the transmitter. However, to be implemented in real time, the exact CSI needs to be acquired at the transmitter, which could be quite challenging due to the power and hardware limitations of passive UHF RFID tags.

In fact, the real challenge with waveform design for UHF RFID systems is to be able to probe the channel without any additional processing or modification at the tag; all processing should be done at the reader. Fortunately, the backscattered wave—highly dependent on the CSI—has the potential for both evaluation and design of RFID systems [11], [12]. In addition, its analytical expressions in free space [13] and multipath [14] propagation environments have been derived. Thus, in frequency diverse single-antenna UHF RFID systems, the observed backscattered signal could be leveraged to acquire some knowledge of the RF channel, adapt power allocation to frequency components, and thereby design channel-adaptive energy efficient waveforms without modifying the tag.

In this work, we propose a waveform design methodology for UHF RFID systems based on the quantitative analysis of the backscattered signal. This latter is leveraged to probe the wireless propagation environment and adapt power allocation to frequency components to improve the energy efficiency of the reader-tag link. RFID system performance is evaluated based on the harvested DC voltage at the output of the rectifying circuit of the tag. For this purpose, we develop an improved hybrid simulation model, first introduced in [15], that accounts for nonlinearities and facilitates studying UHF RFID system performance using optimized waveforms.

The rest of the paper is organized as follows. Section II presents the waveform design methodology. Section III describes the hybrid simulation model developed. Section IV provides performance analysis of the proposed waveforms. Finally, section V draws the conclusion and perspectives.

II. Waveform Design Methodology

A. The Backscattered Wave

Consider a typical amplitude-modulated backscattered RF signal, $r(t)$, received by the reader. Assuming continuous wave (CW) mode transmission (a single sinewave carrier is used at emission) in a lossless, frequency-flat channel, the mathematical expression of such a signal can be written as

$$r(t) = [A + \Delta V m(t)] cos(2\pi F t + \theta) \quad (1)$$

where A represents the constant envelope of the transmit signal received at the reader, $m(t)$ is a binary signal that takes one of two values (0 or 1) each corresponding to a tag load impedance state, F and θ are the carrier frequency and phase of the backscattered signal respectively, and ΔV is the difference in Volts between the averages of the high and low states of backscattered baseband signal. Besides, ΔV is proportional to the magnitude of the Differential RCS (Radar Cross Section) vector as seen from the reader [11]. Thus, after demodulating and filtering $r(t)$, $\Delta V m(t)$ would represent the tag's backscattered baseband signal received at the reader; that is, tag information.

In the presence of multipath fading and frequency-selective channels, $\Delta V m(t)$ can be written as a function of the transmitted signal, the time-varying load reflection coefficient of the RFID tag and the frequency response of the RF channel [14]. From (1), it is inferred that any attenuation induced by the channel's amplitude would influence the quantity $\Delta V m(t)$. Consequently, given its dependency on the CSI, $\Delta V m(t)$ can be utilized to probe the wireless channel. Knowing that A could be filtered out from $r(t)$ using basic digital signal processing (DSP) techniques, ΔV could then be easily calculated and utilized to determine the best communication frequencies based on the two-way link. Therefore, channel-adaptive waveforms could be designed based on the ΔV criterion.

B. Designing Adaptive Multisines Based on Backscattered Wave Analysis

Consider a general multisine signal consisting of a set of N uniformly spaced frequencies, its time-domain expression is given by

$$x(t) = \Re\left\{ \sum_{n=1}^{N} a_n e^{j\phi_n} e^{j2\pi f_n t} \right\} \tag{2}$$

where n is a positive integer ($n \in [1, N]$), and a_n, f_n and ϕ_n are the amplitude, frequency and phase of the n^{th} sinusoid, respectively. The uniformly spaced frequencies are expressed as

$$f_n = f_1 + (n-1)\Delta_f \tag{3}$$

where f_0 is the initial frequency and Δ_f is the frequency spacing. Let $x_n(t)$ be the n^{th} sinusoid, i.e. a CW mode signal having a frequency f_n.

The waveform design methodology consists of, first, evaluating each f_n according to the ΔV criterion during the channel probing phase, then, sorting these frequencies in a decreasing order of ΔV, and last, constructing $x(t)$ by allocating power to the best f_n components. During the channel probing phase, first, $x_n(t)$ is transmitted at each f_n in the operating bandwidth. Then, each respective $r_n(t)$ received by the reader is processed to recover the corresponding baseband signal (at the corresponding frequency) and calculate the corresponding ΔV. This leads to obtaining a ΔV curve as a function of f_n. Based on this curve, the frequencies are sorted according to their ΔV performance: the frequencies corresponding to the highest (resp. lowest) ΔV value are considered as the most (resp. least) favorable operating frequencies. The result is a set of N operating frequencies arranged from the most to the least favorable (or equivalently, from the least to the most attenuated) as seen from the reader. Finally, using (2), a total of N combinations of multisine signals could be created, ranging from 1 frequency per multisine to N frequencies per multisine.

III. Hybrid Simulation Model

To test the previously described waveform design methodology, we rely on an improved hybrid simulation model (first introduced in [15]) of a passive RFID system. The improved model, developed via the ANSYS platform, facilitates studying RFID system performance using unconventional waveforms with a high degree of flexibility and provides access to raw signals at both the reader and tag. By decoupling in time the tag's main functions, the model allows analysing the backscattered signal at the reader and evaluating the harvested energy at the tag.

In a typical passive UHF RFID system, the tag circuit performs three main functions: energy harvesting, demodulation and control logic, and backscatter modulation. Accurately modelling such a tag circuit is particularly challenging because of the design complexity, which is subject to extremely low power constraint. Fortunately, in the case of waveform design, it is sufficient to consider only two of the aforementioned functions performed by the tag: energy harvesting (to evaluate the energetic performance) and backscatter modulation (to generate and analyse the backscattered signals). For simplicity, the energy harvesting and backscatter modulation functions are modelled independently.

The hybrid simulation model is developed using ANSYS Circuit Designer and HFSS co-simulations. Fig. 1 shows a schematic depiction of the simplified UHF RFID system considered in this study. The reader is emulated by a transceiver in a *monostatic* configuration with a single antenna Ant_R while the tag is emulated by a tag circuit and antenna Ant_T. The reader circuit consists of an arbitrary waveform generator (AWG), a circulator, a DC-block capacitor C_{bs}, a resistive load R_{bs}, and a DSP block. The tag circuit consists of two subcircuits that are simulated separately: energy harvester (EH) and backscatter modulator (BM). When the EH is connected to Ant_T, the BM does not interfere with the operation of the tag (completely disconnected), and vise versa when the BM is connected to Ant_T. The first consists of a rectifying circuit and an output resistive load $R_{L_{EH}}$ optimized to maximize the harvested energy, while the second consists of an RF switch, an independent DC voltage source generating a predefined square signal to drive the switch, and a resistive load $R_{L_{BM}}$ matched to the tag antenna.

IV. Performance Analysis

To have a broader perspective on system performance with respect to the different UHF standards present worldwide, the study is carried out on a wide frequency span: from 800 MHz

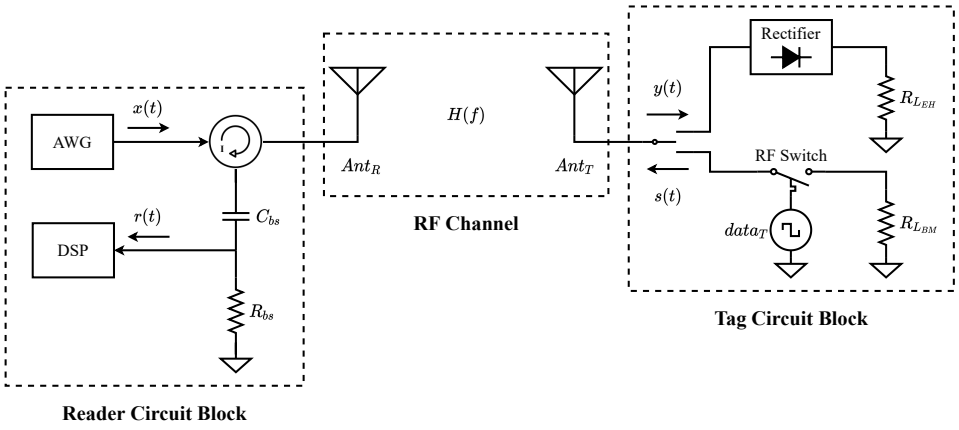

Fig. 1: Schematic depiction of the modeled UHF RFID system.

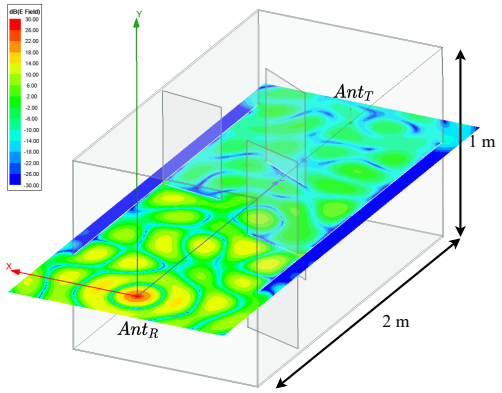

Fig. 2: 3D electromagnetic model: Reader and tag antennas separated by an NLOS propagation environment.

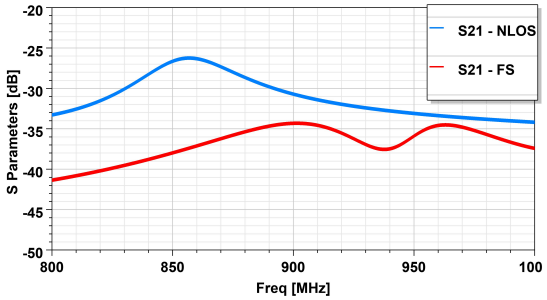

Fig. 3: S21 parameters for NLOS and FS scenarios.

to 1000 MHz, where $f_1 = 800\ MHz$ and $\Delta_f = 10\ MHz$. Thus, a total of $N = 21$ equally spaced frequencies are considered. The average power incident to Ant_R is set to the same constant value, P_t, in all cases.

A. Simulated Scenarios

A typical 50-Ω half-wave dipole antenna is used for both Ant_R and Ant_T. Two channel scenarios are considered: non-line-of-sight (NLOS) and free space (FS). In the NLOS case, a highly reflective propagation environment composed of a rectangular aluminium box in which metallic obstacles have been arbitrarily placed is used. Fig. 2 illustrates one realization of the NLOS scenario where the total electric field lines distribution in the XZ plane at 915 MHz is shown. Fig. 3 shows the frequency response (S21 parameter) corresponding to both scenarios.

B. Channel Probing Phase

To probe the channel, after transmitting $x_n(t)$ at each f_n of the N frequencies, the received $r_n(t)$ is I/Q demodulated and the corresponding ΔV value is obtained. Fig. 4 shows the ΔV values as a function of f_n for both scenarios. These results indicate that the maximum ΔV values are obtained around 860 MHz for the NLOS scenario, and around 940 and 960 MHz for the FS scenario. Looking back at Fig. 3, the S21 parameter shows maximum transmission at around 860 MHz for the NLOS scenario, and around 910 and 960 MHz for the FS scenario. Although not perfectly aligned, it is clear that there exists a strong correlation between the curve profile of ΔV as a function of f_n and the S21 curves as a function of frequency for both scenarios. Of course, the mismatch between both curves is certainly related to the unpredictable phase behaviour of the backward channel. However, this does not undermine the fact that ΔV is a good and reliable indicator of the channel strength.

C. Energetic Performance Evaluation

The energetic performance of the designed waveforms is evaluated based on the RMS value of the DC voltage V_{Load} collected at the output of the rectifying circuit, i.e. at the terminals of $R_{L_{EH}}$ (see Fig. 1). Note that the average transmit power is set to P_t for all emitted signals $x(t)$. For a given N, ϕ_n is set to 0 and the individual sinewaves are set to have equal amplitudes ($a_n = constant$) such that the average transmit power of $x(t)$ is P_t. Fig. 5 illustrates the harvested DC voltage of the designed waveforms as a function of N for both scenarios.

It is noticed that in FS, the harvested energy is maximum for $N = 1$, whereas in the NLOS case, the harvested energy reaches a maximum for $N = 3$. After reaching the peak,

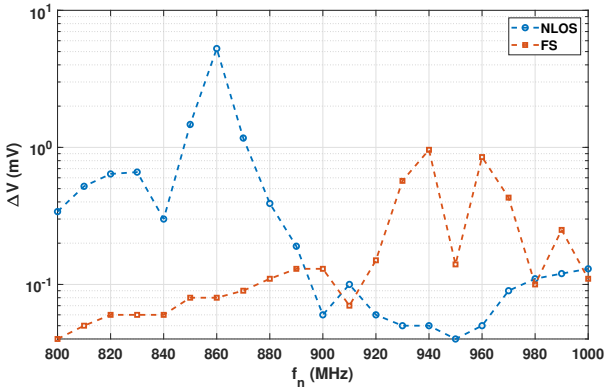

Fig. 4: ΔV values of the baseband signals obtained in CW mode as a function of f_n for NLOS and FS scenarios.

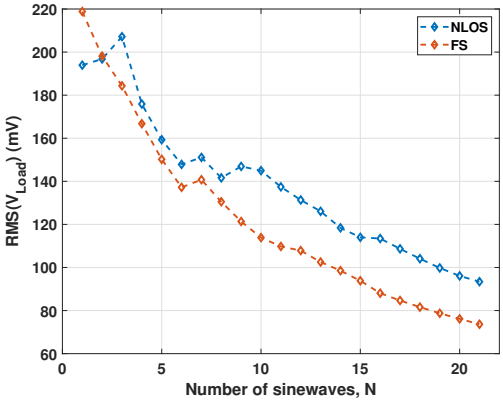

Fig. 5: DC voltage (RMS value) of the designed waveforms collected at the output of the energy harvesting circuit as a function of N for NLOS and FS scenarios.

both curves then decrease gradually as a function of N. In qualitative terms, these results show that the waveforms designed according to backscattered signal analysis improve the energetic performance of the reader-tag link. For the FS scenario, the highest energy is harvested by using a CW signal, while for the NLOS scenario, the highest energy is harvested by using a multisine waveform. This is mainly because the rectifying circuit has been optimized for CW mode operation, which is the case for commercial RFID tags. It is worth noting that using this method, the harvested energy is maximized for the same frequencies that maximize ΔV, meaning that the detection of backscattered information is also improved. Although the obtained results depend strongly on the simulated scenarios and the implemented EH circuit, they still suggest that channel-adaptive multisines that maximize the harvested energy could be designed based on backscattered signal analysis especially in highly reflective environments.

V. Conclusion

In this work, we studied waveform design in UHF RFID systems based on the quantitative analysis of the backscattered signal. The proposed methodology allowed acquiring knowledge on the wireless propagation channel using the backscattered RFID tag information; no additional processing at the tag was needed. Channel-adaptive multisine signals were designed and their energetic performance was evaluated using a flexible and accurate hybrid simulation model. The results showed that the proposed multisines improve the energetic efficiency of the RFID communication link especially in highly reflective environments. Finally, it is worth noting that although the study is limited to two channel scenarios, the methodology could nevertheless be generalized and applied to any possible scenario. In future work, a generalized waveform design algorithm based on backscattered signal analysis will be proposed. In such case, the designed waveforms will be applied to different channels, circuit designs and antennas.

References

[1] Y. Duroc and S. Tedjini, "RFID: A key technology for Humanity," *Comptes Rendus Physique*, vol. 19, no. 1, pp. 64–71, Jan. 2018.

[2] "EPCglobal, EPC (TM) Radio-Frequency Identity Protocols Generation-2 UHF RFID Standard, Specification for RFID Air Interface Protocol for Communications at 860 MHz – 960 MHz, Version 2.1," Jul. 2018.

[3] M. S. Trotter and G. D. Durgin, "Survey of range improvement of commercial RFID tags with Power Optimized Waveforms," in *2010 IEEE International Conference on RFID (IEEE RFID 2010)*, Orlando, FL, USA, Apr. 2010, pp. 195–202.

[4] A. S. Boaventura and N. B. Carvalho, "Maximizing DC Power in Energy Harvesting Circuits Using Multisine Excitation," in *2011 IEEE MTT-S International Microwave Symposium*, Baltimore, MD, USA, 2011, pp. 1–4.

[5] A. Collado and A. Georgiadis, "Optimal Waveforms for Efficient Wireless Power Transmission," *IEEE Microw. Wireless Compon. Lett.*, vol. 24, no. 5, pp. 354–356, May 2014.

[6] B. Clerckx and E. Bayguzina, "Waveform Design for Wireless Power Transfer," *IEEE Trans. Signal Process.*, vol. 64, no. 23, pp. 6313–6328, Dec. 2016.

[7] ——, "Low-Complexity Adaptive Multisine Waveform Design for Wireless Power Transfer," *IEEE Antennas Wireless Propag. Lett.*, vol. 16, pp. 2207–2210, 2017.

[8] M. R. V. Moghadam, Y. Zeng, and R. Zhang, "Waveform Optimization for Radio-Frequency Wireless Power Transfer : (Invited paper)," in *2017 IEEE 18th International Workshop on Signal Processing Advances in Wireless Communications (SPAWC)*, Sapporo, Japan, Jul. 2017, pp. 1–6.

[9] Y. Merakeb, H. Ezzeddine, J. Huillery, A. Bréard, R. Touhami, and Y. Duroc, "Experimental Demonstration of a Passive UHF RFID Communication in Time Reversal and Pulsed Wave Mode," in *2019 IEEE International Conference on RFID Technology and Applications (RFID-TA)*, Pisa, Italy, Sep. 2019, pp. 58–62.

[10] ——, "Experimental platform for waveform optimization in passive UHF RFID systems," *Int J RF Microw Comput Aided Eng*, vol. 30, no. 10, Oct. 2020.

[11] F. Fuschini, C. Piersanti, F. Paolazzi, and G. Falciasecca, "Analytical Approach to the Backscattering from UHF RFID Transponder," *IEEE Antennas Wireless Propag. Lett.*, vol. 7, pp. 33–35, 2008.

[12] G. Yang, C. K. Ho, and Y. L. Guan, "Multi-antenna Wireless Energy Transfer for Backscatter Communication Systems," *IEEE J. Sel. Areas Commun.*, vol. 33, no. 12, pp. 2974–2987, Dec. 2015.

[13] Z. Fan, S. Qiao, J. T. Huang-Fu, and L. Ran, "Signal descriptions and formulations for long range UHF RFID readers," *Proceedings of Progress In Electromagnetics Research Symposium*, pp. 109–127, 2007.

[14] J. D. Griffin and G. D. Durgin, "Multipath Fading Measurements at 5.8 GHz for Backscatter Tags With Multiple Antennas," *IEEE Trans. Antennas Propag.*, vol. 58, no. 11, pp. 3693–3700, Nov. 2010.

[15] H. Ezzeddine, Y. Merakeb, J. Huillery, A. Bréard, Y. Duroc, and C. Vollaire, "Simulation Framework for Studying UHF RFID Systems in Pulse Wave Mode," in *2019 IEEE International Conference on RFID Technology and Applications (RFID-TA)*, Pisa, Italy, Sep. 2019, pp. 120–124.